Responses to Reviewer #3

Journal: Atmospheric Chemistry and Physics

Manuscript Number: egusphere-2025-3956

Title: Response relationship between atmospheric O_3 and its precursors in Beijing based on smog chamber simulation and a revised MCM model

We sincerely appreciate the your careful review and valuable guidance. The manuscript has been thoroughly revised according to your suggestions, and all changes have been clearly highlighted using the Track Changes mode in the revised version. Enclosed please find our point-by-point responses to your comments for your kind consideration.

Responses to your comments

This manuscript presents the relationship between O_3 and its precursors using smog chamber experiments and a revised MCM box model. The authors improve O_3 simulation by accounting for chamber wall effects under experimental conditions and unidentified NO_2 sinks under ambient conditions, highlighting the sensitivity of O_3 formation to VOCs and the implications for mitigation strategies in Daxing, Beijing.

However, the mechanisms related to chamber wall effects appear to have negligible influence when applied to real atmospheric conditions, whereas the unidentified NO2 sinks required for model-measurement agreement are unrealistically large. As a result, the revisions offer limited insights for ambient applications. Moreover, the simplified mechanisms used in the box model do not adequately represent interactions with meteorology or emissions. Therefore, I do not recommend the publication of this paper in ACP.

Response: We appreciate your meticulous evaluation. The impact of ground-mediated reactions on O_3 has been sparsely documented in previous literature. Although our results indicate a minimal influence, we

contend that this finding is scientifically significant as it characterizes a previously unrecognized aspect of O_3. 1D models often encounter substantial uncertainties when resolving complex meteorological dynamics and emission profiles. Given the vast extent of the Earth's surface, the conclusions derived from our model are of significant reference value. Regarding the NO_2 sink, the following revisions have been implemented. Previously, we attempted to simultaneously use NO and NO_2 as constraints. Under that configuration, the impact of varying physical dilution rates on O_3 simulation results was indeed minimal (as illustrated in the Figure R1), which led us to overlook the significance of the physical dilution process in the earlier stages of our study. However, as discussed in the revised manuscript, to more accurately evaluate the influence of ground-related reactions on O_3 formation, we transitioned to a more scientific setup where only NO is constrained. Under this revised configuration, the physical dilution rate exhibits a significant impact on the O_3 simulation results, as detailed in the Figure R2 of the manuscript. However, due to the lack of glyoxal and boundary layer data, a simplified 24-h loss lifetime was employed to evaluate the sensitivity (Figure R2). Our results indicate that while physical processes exert a profound influence on the simulated O_3, the impact of ground-mediated reactions is negligible (Figure R2). We have realized that neglecting physical processes in ambient atmospheric simulations is inappropriate, as it was the primary cause for the previous discrepancies where simulated NO_2 and O_3 concentrations deviated significantly from observations. However, the challenges in accurately characterizing atmospheric physical processes prevent further investigation into O_3 simulation performance, VOCs simulation performance and O_3 sensitivity (EKMA). Consequently, the focus of this study was shifted toward a systematic evaluation of the impact of ground-related reactions on the formation of O_3 and HONO. We conclude that ground-mediated reactions exert a significant influence on HONO, whereas their impact on O_3 is negligible. Detailed modifications have been implemented after line 296.

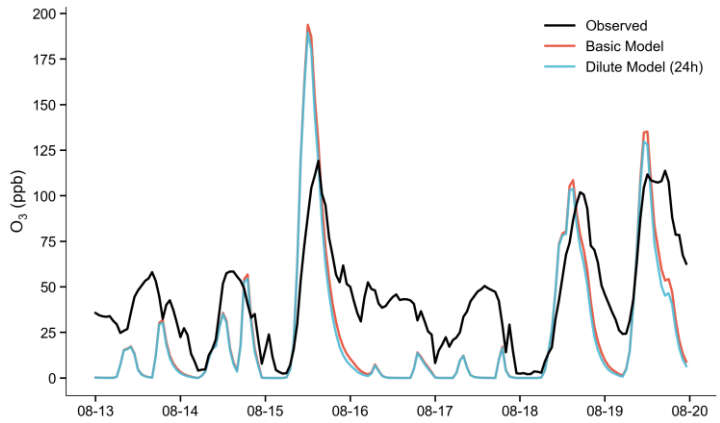

Figure R1. Comparison of observed and simulated O_3 concentrations across different model scenarios. The base model results were obtained with NO and NO_2 concentrations constrained. The dilute model results reflect the impact of a 24 h physical dilution process on the simulated O_3 levels.

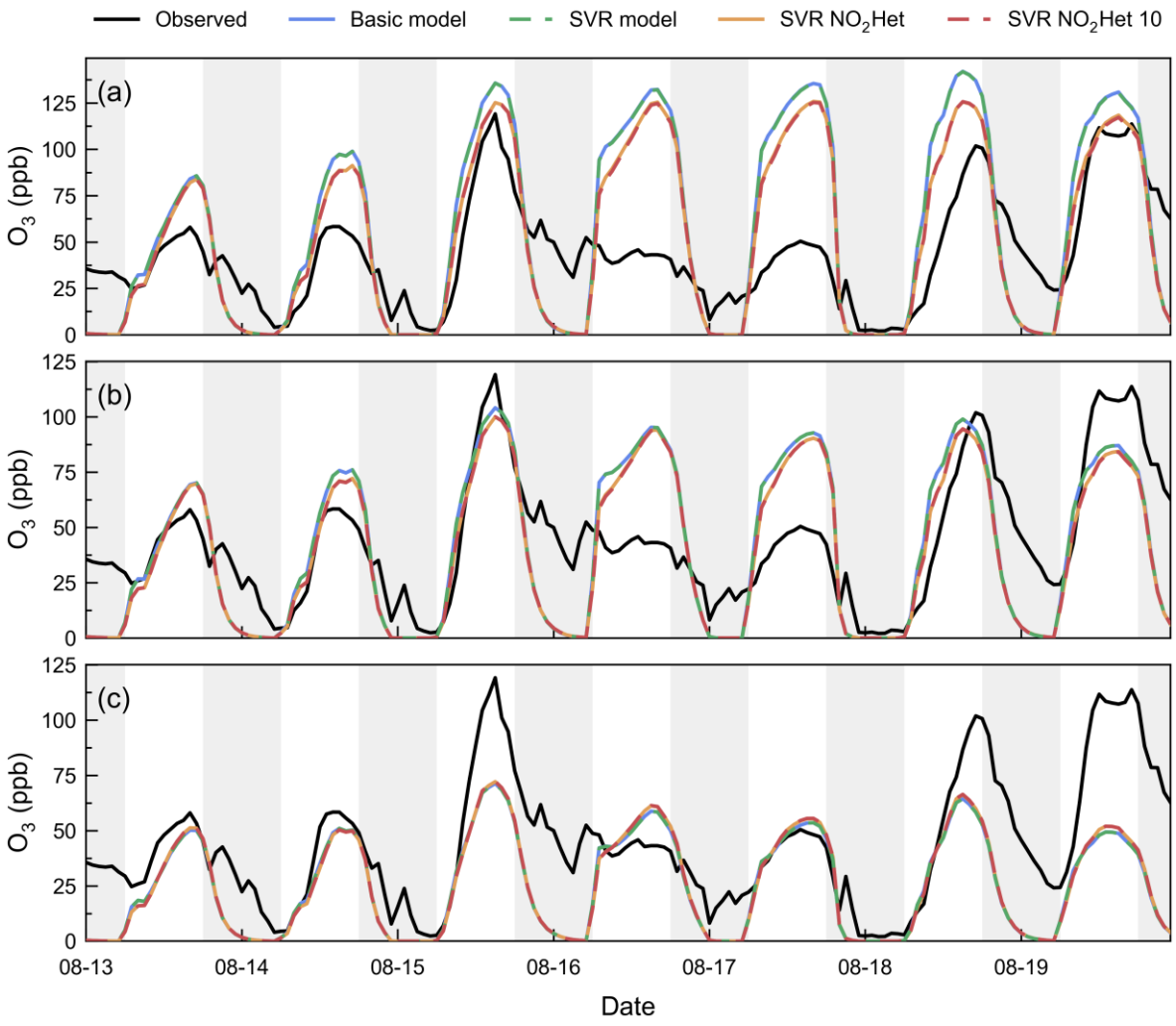

Figure R2. Comparison of observed and simulated O_3 concentrations under physical dilution rates of (a)

5.80×10^{-6} s^{-1}, (b) 1.16×10^{-5} s^{-1} and (c) 2.32×10^{-5} s^{-1}. The black curves represent the observed O_3 concentrations, and the shaded areas denote nighttime periods. Compared to the basic model, the SVR model incorporates ground-related reaction mechanisms derived from chamber experiments. The SVR NO_2Het model further adjusts the ground-related NO_2 heterogeneous reactions based on the SVR model. In the SVR NO_2Het 10 model, the rates of all reactions, excluding the NO_2 heterogeneous reactions, are scaled up by a factor of 10 relative to the SVR NO_2Het model.

Major Comments

1. The revised model (O_3 SVR) shows better agreement with chamber results than the base model, primarily due to the introduction of ·OH generation associated with chamber wall effects. While such a mechanism may be justified within a chamber, there is minimal physical basis for applying this wall-induced radical source to ambient atmospheric conditions. Ground-related reactions on atmospheric chemistry do not mimic chamber wall reactions, and extending this mechanism to the atmosphere is inappropriate.

Response: After a thorough reassessment, we entirely concur with your perspective that the direct extrapolation of wall-induced OH radical sources from smog chambers to complex ambient atmospheric conditions lacks a solid physical basis.

Revised text as it appears in line 267-269 of the text:

However, the source mechanisms of OH radicals and the conversion of ·OH to HO_2 appear to be chamber-specific. Incorporating these incomplete mechanisms into models for simulating ambient conditions is inappropriate and lacks physical basis.

2. Reaction rate constants associated with wall effects in Table 2 are key parameters, but their optimization

process is insufficiently described (Page 6, Line 159; Page 7, Line 162 and Line 167). For example, how the reported J_{NO2} = 0.0015 ppbv s^{-1} (range 0.00075-0.0030 ppbv s^{-1}) in Angove et al. is converted to 1.2 × 10^6 molecule cm^{-3} s^{-1} in this study (reaction 1: hv + wall → ·OH).

Response: At standard temperature and pressure, 1 ppb is equivalent to 2.46 × 10^{10} molecules cm^{-3} which allows the unit of the reported rate to be converted to molecules cm^{-3} s^{-1}. Additional details regarding the specific optimization process have been included in the revised manuscript.

Revised text as it appears in line 183-196 of the text:

To achieve optimal model performance for VOCs across all experimental cases, the OH radical source rate constant reported by Wang et al. (2014) was adjusted within an order of magnitude (Wang et al., 2014). Following iterative optimization, the final OH production rate constant was determined to be 1.2 × 10^6 molecules cm^{-3} s^{-1}. Meanwhile, the mechanism of light-induced release of NO_2 from the wall (Bloss et al., 2005; Carter and Lurmann, 1991) was introduced to address the issue of relatively low production of NO_2 in the simulation. The NO_2 source rate constant from Wang et al. (2014) was varied within an order of magnitude. Through iterative optimization, the optimal NO_2 release rate constant was determined to be 6 × 10^5 molecules cm^{-3} s^{-1}, which is intermediate between the values reported by Angove et al. (Hynes et al., 2005) and Wang et al. (Wang et al., 2014). In addition, Teflon wall can release small amounts of organic impurities, which will consume OH radicals and generate HO_2 radicals (Metzger et al., 2008). Therefore, the additional mechanism that converts OH radicals into HO_2 radicals was also introduced into the model. This mechanism can accelerate the consumption of NO and also compensating for the deficiency of the simulated NO_2 and O_3 concentration. The relevant rate constants from Carter and Lurmann (1991) were varied within an order of magnitude. Through iterative optimization, the optimal conversion rate constant of OH radicals to HO_2 radicals is determined to be 10 s^{-1}, which lies within the range mentioned by Carter and Lurmann (Carter and Lurmann, 1991).

The optimized rate constants may be chamber-specific. A controlled validation experiment using a small, clean plastic chamber (e.g., 1 m^3) under similar conditions is therefore recommended. Is the revised model, with these parameters, able to reproduce results from such test-chamber conditions?

Response: We acknowledge that wall effects and their corresponding rate constants exhibit significant variations across different smog chambers, a phenomenon that has been well-documented in previous studies (Hynes et al., 2005; Metzger et al., 2008; Wang et al., 2014). Therefore, within our current research framework, we maintain that conducting iterative optimization for the wall effects specific to our smog chamber is a robust and effective approach to ensure the reliability of the model parameters.

Upper and lower limits for relevant parameters should also be provided, and a sensitivity analysis is recommended to assess how uncertainties in each parameter affect model-measurement discrepancies.

Response: It has been revised accordingly. The results of the sensitivity analysis are shown in Figure S5.

Revised text as it appears in line 220-225 of the text:

Furthermore, sensitivity analyses for individual wall-related reactions were conducted based on the Iso&Tol02 and Iso&Tol04 experiments (Fig. S5) to quantify the influence of parameter uncertainties on model performance. The results indicate that the OH radical source mechanism and the OH-to-HO_2 conversion pathway exert substantial influence on the simulated O_3 concentrations. In contrast, the NO_2 source mechanism, NO_2 heterogeneous reactions, and O_3 wall loss show moderate impacts, while the remaining reactions have limited effects on the O_3 simulation results.

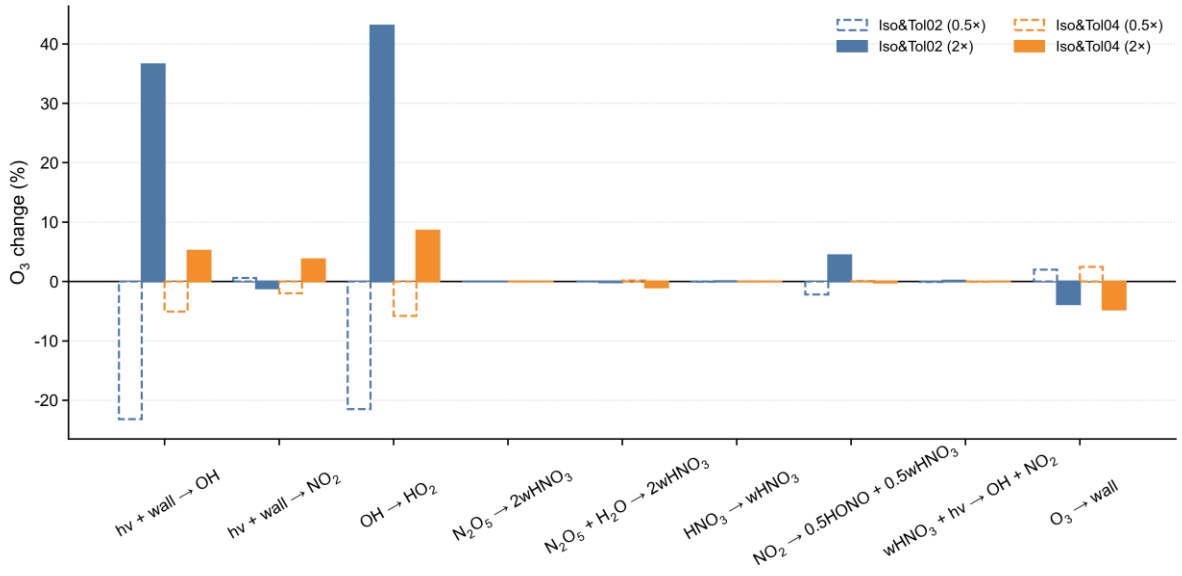

Figure S5: Sensitivity of simulated maximum O_3 concentrations to variations in reaction rate constants for experiments Iso&Tol02 and Iso&Tol04. The percentages represent deviations from the base simulation using a model incorporated with wall effect mechanisms. Most reaction rates were scaled by factors of 2 and 0.5, while the $N_2O_5 + H_2O$ reaction rate was specifically adjusted by factors of 10 and 0.1.

1. Other experiments beyond Iso&Tol02 and Iso&Tol04 should be briefly described in the Supplement, including their experimental design and key results beyond simply displaying NMB values (Page 8, Line 185).

Response: It has been revised accordingly.

Revised text as it appears in line 144-152 of the text:

To investigate the effect of precursor and chamber wall loss on O_3 formation, a series of experiments were conducted with varying precursor concentrations. In the mixed systems, results from Iso&Tol01, Iso&Tol02, and Tol01 demonstrated that O_3 production exhibited a decreasing trend as isoprene concentrations declined (Fig. 1, Fig. S4, and Table 1). Similarly, experiments Iso&Tol01, Iso&Tol03, and Iso01 showed that O_3

formation decreased with a reduction in toluene concentration (Fig. S4 and Table 1). For the Iso&Tol01, Iso&Tol04, and Iso&Tol05 series, O_3 production initially increased and subsequently decreased as NO_x concentrations were reduced (Fig. 1, Fig. S4, and Table 1). In single VOC systems, experiments Iso01 and Iso02 indicated an increase in O_3 formation with higher isoprene concentrations. These observed relationships between O_3 and its precursors are consistent with established atmospheric chemistry theory, underscoring the reliability of our experimental results.

2. The authors introduced a constant NO_2 sink to correct the model-measurement bias (Page 12, Line 270). However, the magnitude of this sink lacks physical justification and may simply force agreement for the wrong reasons. The authors should discuss alternative explanations for the observed bias beyond invoking an NO_2 uptake, and evaluate whether other processes could plausibly account for the discrepancy.

Response: As previously stated, physical processes exert a substantial influence on the simulation results. These processes significantly modulate O_3 formation, thereby partially accounting for the systematic overestimation of O_3 and NO_2 relative to observations in earlier modeling studies.

3. The attribution of O_3 overestimation in the SVR NO_2-sink model on 16-17 Aug to prevailing winds and associated air mass changes (Page 12, Line 277) requires further validation. The model overestimates O_3 continuously from late afternoon on Aug 15 through early morning Aug 16, during which wind speed decreased by more than a factor of four. Statistical analysis is needed to support the proposed explanation.

Response: The mean wind speed during 15–17 was 2.31 m/s, whereas it averaged 1.76 m/s during other periods. We attribute the significant decrease in NO_2 concentrations during the night to air mass replacement events that occurred over these three days. Since 0-D box models are inherently unable to capture transport

processes such as air mass changes, the model could not predict this sharp decrease in NO_2. Consequently, this led to an overestimation of daytime O_3 concentrations in our simulations.

Minor Comments

1. Subtitles for each section should be more concise.

Response: It has been revised accordingly.

The new subtitles are as follows:

Line 143: 3.1 Construction of a revised model

Line 211: 3.2 Evaluation of the revised model

Line 226: 3.3 Impact of the revised model on the sensitivity of O_3

Line 244: 3.4 Ambient application of the revised model

Line 296: 3.5 Further revision of the model

2. Table 1. Please explain why $NO_{x,0}$ is even lower than NO_0 under some experimental conditions?

Response: These initial concentrations were measured using the Thermo 42i analyzer. In some cases, when NO_2 concentrations were below the detection limit, the instrument recorded negative values, which resulted in the calculated NO_x concentrations being lower than NO. We have corrected the NO_x concentrations in Table 1 to address this issue.

3. Please clarify what J1-J56 correspond to in Table S1, and explain why J4 is selected in AtChem2-MCM in Table S2 (Supplement Page 6).

Response: J1–J8 represent the photolysis rate constants for inorganic species, while J11–J56 correspond to

those for organic species. Collectively, these parameters reflect the spectral characteristics of the light source. The detailed correspondence between these constants and specific chemical species has been further clarified in Table S1 of the Supplementary Material. For more comprehensive information, please refer to the MCM official website. Specifically, J4 refers to the photolysis rate constant of NO_2, which is a core parameter governing tropospheric O_3 formation. Given that J4 directly determines the chemical production rate of O_3, its accuracy is critical. In our model simulations, we derived a photolysis scaling factor, JFAC, by comparing measured J4 values with their theoretical values. All other photolysis constants (J1–J56) were then synchronized using this factor to ensure that the simulated environment closely matches the actual light conditions.

Table S1: Photolysis rate constants used in the MCM box model for simulating smog chamber experiments.

J	Species	Value (s-1)	J	Species	Value (s-1)	J	Species	Value (s-1)
J1	O3	1.05E-05	J2	O3	2.52E-06	J3	H2O2	4.85E-06
J4	NO2	9.20E-03	J5	NO3	2.17E-05	J6	NO3	5.37E-05
J7	HONO	2.03E-03	J8	HNO3	5.66E-07	J11	HCHO	1.94E-06
J12	HCHO	2.20E-06	J13	CH3CHO	9.73E-07	J14	C2H5CHO	1.61E-06
J15	C3H7CHO	5.20E-07	J16	C3H7CHO	2.48E-07	J17	IPRCHO	2.31E-06
J18	MACR	5.12E-07	J19	MACR	5.12E-07	J20	C5HPALD1	2.63E-04
J21	CH3COCH3	3.10E-07	J22	MEK	2.81E-07	J23	MVK	3.08E-07
J24	MVK	3.08E-07	J31	GLYOX	5.62E-07	J32	GLYOX	5.17E-06
J33	GLYOX	3.24E-05	J34	MGLYOX	3.85E-05	J35	BIACET	7.34E-05
J41	CH3OOH	4.56E-07	J51	CH3NO3	9.22E-07	J52	C2H5NO3	1.76E-07
J53	NC3H7NO3	2.71E-04	J54	IC3H7NO3	2.86E-04	J55	TC4H9NO3	1.08E-06
J56	NOA	7.26E-06						

4. Units should be provided for all variables in equations (1) and (2).

Response: It has been revised accordingly.

Revised text as it appears in line 106-109 and 263-265 of the text:

In the Eq. (1), the actinic flux I (photons cm^{-2} s^{-1} nm^{-1}) is used to characterize the distribution of light intensity within the smog chamber. The absorption cross section σ (cm^2 $molecule^{-1}$) and the quantum yield Φ (dimensionless) describe the molecular light absorbing properties and energy conversion efficiency, respectively, during photolysis. And lambda is the wavelength (nm).

where k (s^{-1}) is defined as the surface reaction rate constant for HONO, γ (dimensionless) represents the uptake coefficient, v_{NO_2} ($m \cdot s^{-1}$) denotes the average molecular velocity of NO_2, and S/V_g (m^{-1}) stands for the surface-to-volume ratio of the ground.

5. Please discuss whether effects other than wall loss may contribute to model-measurement discrepancies (Page 6, Line 144).

Response: Thanks for your valuable suggestion. You are correct to highlight that discrepancies between model simulations and measurements are often multi-factorial. While we focused on analyzing the role of wall loss as a specific, often dominant factor in chamber-influenced scenarios, we acknowledge that a combination of the factors, such as the uncertainties in reaction rate constants, product yields, and the representation of heterogeneous or multiphase processes, contributes to the model-measurement discrepancies. It has been revised accordingly.

Revised text as it appears in line 166-169 of the text:

While we focused on analyzing the role of wall loss as a specific, often dominant factor in chamber-influenced scenarios, we acknowledge that a combination of the factors, such as the uncertainties in reaction rate constants, product yields, and the representation of heterogeneous or multiphase processes, contributes to the model-measurement discrepancies.

6. Figure 1. Please explain why, despite the large base-model/measurement differences for both Iso&Tol02 and Iso&Tol04 throughout the process, the base-model/measurement difference at 6 h is much smaller for Iso&Tol04 than for Iso&Tol02?

Response: The differences in simulation bias illustrated in Figure 1 primarily arise from the significantly distinct initial NO concentrations between the two experimental cases. In Iso&Tol02, the extremely high initial NO concentration led to intense O_3 titration reactions in the basic model. Furthermore, the wall effect leads to an increase in actual O_3 concentrations, a phenomenon that the basic model fails to capture. Both phenomena collectively lead to the significant discrepancy between the simulated and observed O_3 concentrations in Iso&Tol02. In contrast, the NO concentration in Iso&Tol04 was lower, and the titration effect was relatively weaker; thus, the simulation results from the basic model were more consistent with the observations.

7. Figure 2 and Figure 4. Using a consistent colorbar range across subplots is recommended to improve comparability.

Response: It has been revised accordingly.

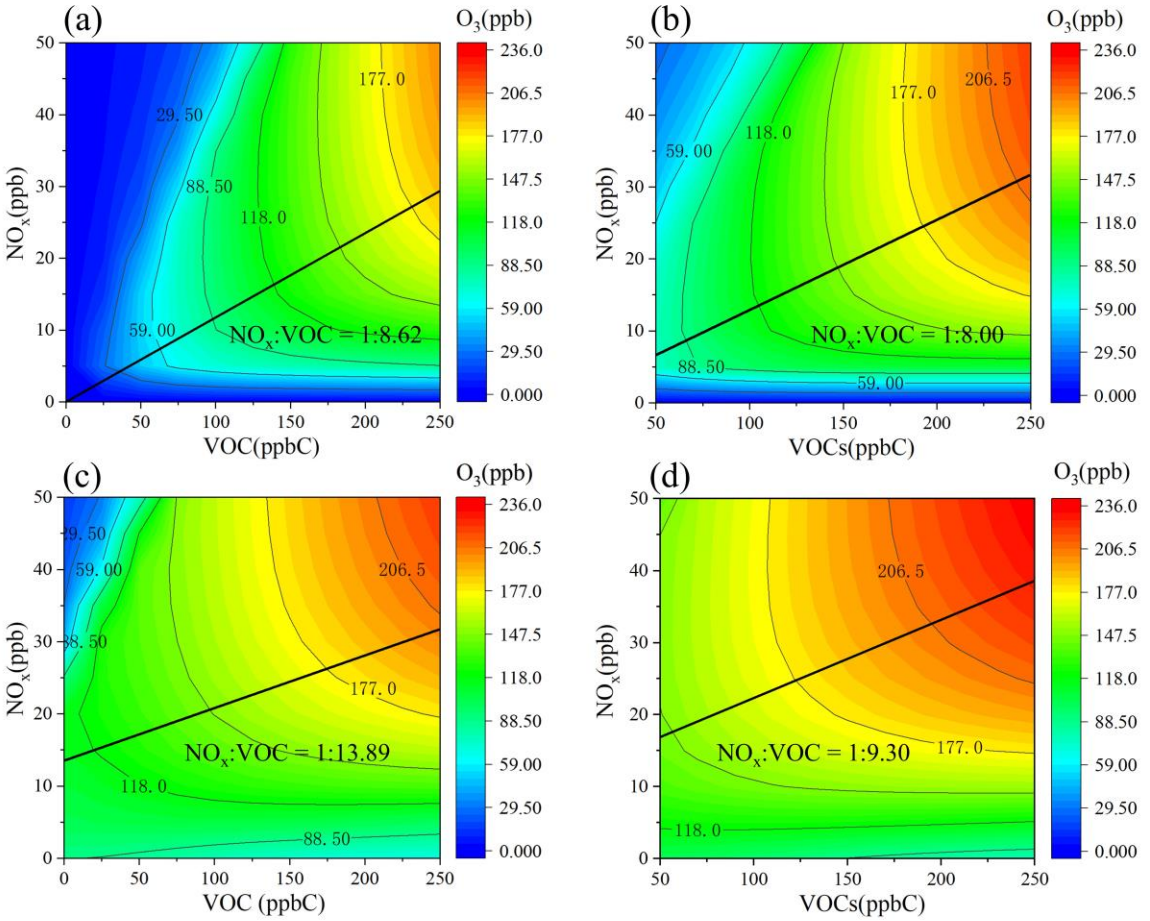

Figure 2: Simulated EKMA curves for O_3 generation under the (a) toluene only system and (b) mixed VOCs system using the basic model. Correspondingly, (c) and (d) display the simulated EKMA curves for O_3 generation under the toluene only system and mixed VOCs system, respectively using the revised model.

8. Table 3. Please clarify whether 0.007 s^{-1} represents J_{NO2} at noon and provide full definitions for k_{gn}, k_{an}, S_a, and other variables.

Response: Regarding the parameter settings in Table 3, we have updated the original value from 0.007 s^{-1} to 0.005 s^{-1}, which is a representative value informed by the literature (Liu et al., 2019).

Revised text as it appears in line 317-319 of the text:

γ_g denote the uptake coefficients of NO_2 on ground surface, while γ_{gd} represent the photo-enhanced

uptake coefficients of NO_2 under illuminated conditions for ground. k_{gn} and k_{gd} represent the first-order rate constants for the heterogeneous reaction of NO_2 during nighttime and daytime, respectively.

Technical Corrections

1. Grammar issues should be corrected, including "the complex of atmospheric conditions" (Page 2, Line 39), "studying how secondary pollutants like O_3 formation" (Page 2, Line 48), and "details information" (Page 5, Line 116).

Response: It has been revised accordingly.

Revised text as it appears in line 38-40, 46-47, and 114-115 of the text:

However, the complexity of atmospheric chemical processes poses challenges for accurate characterization, resulting in significant biases in sensitivity analysis of O_3 formation (Li et al., 2018; Xue et al., 2021; Qu et al., 2021; Chen et al., 2024), and triggering debates over optimal precursor control strategies.

Smog chamber has emerged as an indispensable approach for studying the formation of secondary pollutants such as O_3 (Chen et al., 2022; Carter et al., 1995).

The detailed information about this site and measuring instruments can be found in our previous study (Chen et al., 2021; Xuan et al., 2023).

References

Bloss, C., Wagner, V., Bonzanini, A., Jenkin, M. E., Wirtz, K., Martin-Reviejo, M., and Pilling, M. J.: Evaluation of detailed aromatic mechanisms (MCMv3 and MCMv3.1) against environmental chamber data, Atmos. Chem. Phys., 5, 623-639, 10.5194/acp-5-623-2005, 2005.

Carter, W. P. L. and Lurmann, F. W.: Evaluation of a detailed gas-phase atmospheric reaction mechanism

using environmental chamber data, Atmospheric Environment. Part A. General Topics, 25, 2771-2806, https://doi.org/10.1016/0960-1686(91)90206-M, 1991.

Carter, W. P. L., Pierce, J. A., Luo, D., and Malkina, I. L.: Environmental chamber study of maximum incremental reactivities of volatile organic compounds, Atmospheric Environment, 29, 2499-2511, https://doi.org/10.1016/1352-2310(95)00149-S, 1995.

Chen, G., Xu, L., Yu, S., Xue, L., Lin, Z., Yang, C., Ji, X., Fan, X., Tham, Y. J., Wang, H., Hong, Y., Li, M., Seinfeld, J. H., and Chen, J.: Increasing Contribution of Chlorine Chemistry to Wintertime Ozone Formation Promoted by Enhanced Nitrogen Chemistry, Environmental Science & Technology, 58, 22714-22721, 10.1021/acs.est.4c09523, 2024.

Chen, T., Zhang, P., Ma, Q., Chu, B., Liu, J., Ge, Y., and He, H.: Smog Chamber Study on the Role of NOx in SOA and O3 Formation from Aromatic Hydrocarbons, Environmental Science & Technology, 56, 13654-13663, 10.1021/acs.est.2c04022, 2022.

Chen, T., Liu, Y., Ma, Q., Chu, B., Zhang, P., Liu, C., Liu, J., and He, H.: Significant source of secondary aerosol: formation from gasoline evaporative emissions in the presence of SO2 and NH3, Atmos. Chem. Phys., 19, 8063-8081, 10.5194/acp-19-8063-2019, 2019.

Chen, T., Liu, J., Ma, Q., Chu, B., Zhang, P., Ma, J., Liu, Y., Zhong, C., Liu, P., Wang, Y., Mu, Y., and He, H.: Measurement report: Effects of photochemical aging on the formation and evolution of summertime secondary aerosol in Beijing, Atmos. Chem. Phys., 21, 1341-1356, 10.5194/acp-21-1341-2021, 2021.

Hynes, R. G., Angove, D. E., Saunders, S. M., Haverd, V., and Azzi, M.: Evaluation of two MCM v3.1 alkene mechanisms using indoor environmental chamber data, Atmospheric Environment, 39, 7251-7262, https://doi.org/10.1016/j.atmosenv.2005.09.005, 2005.

Li, Q., Zhang, L., Wang, T., Wang, Z., Fu, X., and Zhang, Q.: “New” Reactive Nitrogen Chemistry Reshapes

the Relationship of Ozone to Its Precursors, Environmental Science & Technology, 52, 2810-2818, 10.1021/acs.est.7b05771, 2018.

Liu, Y., Lu, K., Li, X., Dong, H., Tan, Z., Wang, H., Zou, Q., Wu, Y., Zeng, L., Hu, M., Min, K.-E., Kecorius, S., Wiedensohler, A., and Zhang, Y.: A Comprehensive Model Test of the HONO Sources Constrained to Field Measurements at Rural North China Plain, Environmental Science & Technology, 53, 3517-3525, 10.1021/acs.est.8b06367, 2019.

Metzger, A., Dommen, J., Gaeggeler, K., Duplissy, J., Prevot, A. S. H., Kleffmann, J., Elshorbany, Y., Wisthaler, A., and Baltensperger, U.: Evaluation of 1,3,5 trimethylbenzene degradation in the detailed tropospheric chemistry mechanism, MCMv3.1, using environmental chamber data, Atmos. Chem. Phys., 8, 6453-6468, 10.5194/acp-8-6453-2008, 2008.

Qu, H., Wang, Y., Zhang, R., Liu, X., Huey, L. G., Sjostedt, S., Zeng, L., Lu, K., Wu, Y., Shao, M., Hu, M., Tan, Z., Fuchs, H., Broch, S., Wahner, A., Zhu, T., and Zhang, Y.: Chemical Production of Oxygenated Volatile Organic Compounds Strongly Enhances Boundary-Layer Oxidation Chemistry and Ozone Production, Environmental Science & Technology, 55, 13718-13727, 10.1021/acs.est.1c04489, 2021.

Wang, X., Liu, T., Bernard, F., Ding, X., Wen, S., Zhang, Y., Zhang, Z., He, Q., Lü, S., Chen, J., Saunders, S., and Yu, J.: Design and characterization of a smog chamber for studying gas-phase chemical mechanisms and aerosol formation, Atmos. Meas. Tech., 7, 301-313, 10.5194/amt-7-301-2014, 2014.

Wong, K. W., Tsai, C., Lefer, B., Grossberg, N., and Stutz, J.: Modeling of daytime HONO vertical gradients during SHARP 2009, Atmos. Chem. Phys., 13, 3587-3601, 10.5194/acp-13-3587-2013, 2013.

Xuan, H., Zhao, Y., Ma, Q., Chen, T., Liu, J., Wang, Y., Liu, C., Wang, Y., Liu, Y., Mu, Y., and He, H.: Formation mechanisms and atmospheric implications of summertime nitrous acid (HONO) during clean, ozone pollution and double high-level PM2.5 and O3 pollution periods in Beijing, Science of The Total

Environment, 857, 159538, https://doi.org/10.1016/j.scitotenv.2022.159538, 2023.

Xuan, H., Liu, J., Zhao, Y., Cao, Q., Chen, T., Wang, Y., Liu, Z., Sun, X., Li, H., Zhang, P., Chu, B., Ma, Q., and He, H.: Relative humidity driven nocturnal HONO formation mechanism in autumn haze events of Beijing, npj Climate and Atmospheric Science, 7, 193, 10.1038/s41612-024-00745-8, 2024.

Xue, M., Ma, J., Tang, G., Tong, S., Hu, B., Zhang, X., Li, X., and Wang, Y.: ROx Budgets and O3 Formation during Summertime at Xianghe Suburban Site in the North China Plain, Advances in Atmospheric Sciences, 38, 1209-1222, 10.1007/s00376-021-0327-4, 2021.